Journal of Extracellular Vesicles

co-action PUBLISHING

ORIGINAL RESEARCH ARTICLES

MSC secretes at least 3 EV types each with a unique permutation of membrane lipid, protein and RNA

Ruenn Chai Lai[1†], Soon Sim Tan[1†], Ronne Wee Yeh Yeo[1†], Andre Boon Hwa Choo[2,3], Agnes T. Reiner[4], Yan Su[5], Yang Shen[5], Zhiyan Fu[5], Lezhava Alexander[5], Siu Kwan Sze[6] and Sai Kiang Lim[1,7*]

[1]A*STAR Institute of Medical Biology, Singapore; [2]A*STAR Bioprocessing Technology Institute, Singapore; [3]Department of Biomedical Engineering, Faculty of Engineering, NUS, Singapore; [4]BioSensor Technologies, AIT-Austrian Institute of Technology GmbH, Vienna, Austria; [5]A*STAR Genome Institute of Singapore, Singapore; [6]School of Biological Sciences, Nanyang Technological University, Singapore; [7]Department of Surgery, YLL School of Medicine, NUS, Singapore

Mesenchymal stem cell (MSC), a widely used adult stem cell candidate for regenerative medicine, has been shown to exert some of its therapeutic effects through the secretion of extracellular vesicles (EVs). These homogenously sized EVs of 100–150 ηm exhibited many exosome-like biophysical and biochemical properties and carry both proteins and RNAs. Recently, exosome-associated proteins in this MSC EV preparation were found to segregate primarily to those EVs that bind cholera toxin B chain (CTB), a GM1 ganglioside-specific ligand, and pulse-chase experiments demonstrated that these EVs have endosomal origin and carried many of the exosome-associated markers. Here, we report that only a fraction of the MSC EV proteome was found in CTB-bound EVs. Using Annexin V (AV) and Shiga toxin B subunit (ST) with affinities for phosphatidylserine and globotriaosylceramide, respectively, AV- and a ST-binding EV were identified. CTB-, AV- and ST–binding EVs all carried actin. However, the AV-binding EVs carried low or undetectable levels of the exosome-associated proteins. Only the ST-binding EVs carried RNA and EDA-containing fibronectin. Proteins in AV-binding EVs were also different from those released by apoptotic MSCs. CTB- and AV-binding activities were localized to the plasma membrane and cytoplasm of MSCs, while ST-binding activity was localized to the nucleus. Together, this study demonstrates that cells secrete many types of EVs. Specifically, MSCs secrete at least 3 types. They can be differentially isolated based on their affinities for membrane lipid-binding ligands. As the subcellular sites of the binding activities of these ligands and cargo load are different for each EV type, they are likely to have a different biogenesis pathway and possibly different functions.

Keywords: *exosome*; *mesenchymal stem cell*; *cholera toxin B*; *shiga toxin*; *annexin V*

Responsible Editor: Suresh Mathivanan, La Trobe University, Australia.

*Correspondence to: Sai Kiang Lim, Institute of Medical Biology, 8A Biomedical Grove, #05-05 Immunos, Singapore 138648, Singapore, Email: saikiang.lim@imb.a-star.edu.sg

To access the supplementary material to this article, please see Supplementary files under 'Article Tools'.

Received: 22 September 2015; Revised: 17 January 2016; Accepted: 21 January 2016; Published: 24 February 2016

Mesenchymal stem cells (MSCs) are multipotent stem cells that can be prepared from both adult and foetal tissues, or differentiated from human embryonic stem cells (ESCs) and induced pluripotent stem cells (iPSCs). They are the most widely used regenerative stem cell candidate with nearly 500 MSC clinical trials (www.clinicaltrials.gov/; accessed May 2015). The advantages of MSCs are their ease of isolation from many adult tissues (1), prolific *ex vivo* expansion capacity and a diverse differentiation potential. MSC-based cell therapies have generally been proven to be clinically safe. The mechanism of action underpinning the therapeutic efficacy of MSCs remains controversial but has been increasingly attributed to their secretion, which is thought to reduce cellular injury and enhance repair.

Several years ago, our group observed that culture medium conditioned by MSCs was therapeutically efficacious in a pig and mouse model of myocardial ischemia/reperfusion

[†]These authors have contributed equally to the work.

injury (2) and that the therapeutic agents in the conditioned medium were homogenously sized particles with a hydrodynamic radius of 55–65 ηm and a flotation density in sucrose of 1.10–1.18 g/mL (3). They carried exosome-associated proteins such as the tetraspanin proteins CD9 and CD81, ALIX, TSG101 and RNAs of less than 300 nt (4). Based on these characteristics, these particles were identified as exosomes, a specific type of extracellular vesicle (EV). Subsequent analysis including pulse-chase experiments confirmed that the tetraspanin proteins CD9 and CD81, and endosomal markers ALIX and TSG101, were associated primarily with EVs that bind cholera toxin B chain (CTB), and that these CTB-binding EVs were derived from endosomes. They were also enriched in GM1 gangliosides, which are the endogenous receptors for CTB (5).

In this follow up, we observed that only a fraction of the proteins and none of the RNAs present in our so-called exosome preparation were found in MSC CTB-EVs. This suggests that the exosome preparation may contain other EV types. For clarity, our previously reported MSC exosome preparation will be referred to as an MSC EV preparation in this report. To isolate other EVs, we determined whether other membrane lipid-binding ligands could extract the remaining EVs from MSC secretion, and whether these extracted EVs contain unique cargos of proteins and RNA. The rationale for using lipid-binding ligands for EV isolation is that the lipid membrane is the defining and physically delimiting feature of EVs (6). By targeting membrane lipids, this isolation approach not only enriches for lipid membrane-bound entities, but also eliminates contaminating macromolecules.

Here, we tested Annexin V (AV) and Shiga Toxin (ST), 2 proteins known to bind phosphatidylserine and globotriaosylceramide, respectively, for EV extraction. The protein and RNA contents of CTB-, AV- and ST-binding EVs (CTB-EVs, AV-EVs and ST-EVs) were determined and compared. These EVs were visualized by electron microscopy. The subcellular localization of CTB-, AV- and ST-binding activity was determined by confocal microscopy.

Materials and methods

MSC culture

Immortalized E1-*MYC* 16.3 human ESC-derived MSCs were cultured in DMEM with 10% foetal calf serum as previously described (7). For EV preparation, the cells were grown in a chemically defined medium (NCM) for 3 days and the conditioned medium (CM) was harvested and 0.22 μm filtered as previously described (3,8,9). The CM was concentrated 100 × for EVs by tangential flow filtration (TFF) (Sartorius, Gottingen, Germany, MWCO 100 kDa). The EV preparation was filtered with a 0.22 μm filter (Merck Millipore, Billerica, MA) and stored in −20°C freezer until use. The EVs were assayed for protein concentration using Coomassie Plus™ (Bradford) Assay (Thermo Fisher Scientific, Waltham, MA), as per manufacturer's instruction.

Mass spectrometry analysis of protein

The MSC EV preparation described above was extracted with CTB to isolate the CTB-binding EVs as described below. The remaining EV preparation after CTB extraction was collected as CTB-depleted MSC EV. Proteins (250 μg) from each of the 2 fractions were analysed by LC-MS/MS. Briefly, the samples were reduced by DTT, alkylated with IAA, digested by trypsin and analysed with LC-MS/MS as described (10). For each sample, all MS/MS spectra of each of the 3 independent preparations were extracted by ProteomeDiscovere 1.4 (Thermo Scientific, Bremen, Germany) and combined into a single mascot generic file by a hand-written program. Protein identification was achieved by searching the combined data against the Uniprot human protein database (download 22 Jan 2014; 88479 sequences, 35079223 residues) via an in-house Mascot server (Version 2.4.1Matrix Science, UK). The search parameters were a maximum of 2 missed cleavages using trypsin; fixed modification was carbamidomethylation of cysteine, and variable modifications were oxidation of methionine and deamidation of asparagine and glutamine. The mass tolerances were set to 10 ppm and 0.8 Da for peptide precursor and fragment ions, respectively. Protein identification was accepted as true positive if 2 different peptides were found to have scores greater than the homology or identity scores.

EV extraction with CTB, AV and ST

CTB (SBL Vaccin AB, Sweden), AV (Biovision, San Francisco, USA) and ST (Sigma, St Louis, USA) were biotinylated using Sulfo-NHS Biotin (Thermo Fisher Scientific, Waltham, MA) as per manufacturer's instruction; 20 μg MSC EVs prepared as described above were incubated with 0.25 μg biotinylated CTB, AV or ST in binding buffer (100 mM Hepes, 2.5 mM $CaCl_2$, 140 μM NaCl, PBS pH7.4), at a final volume of 100 μL for 30 minutes with rotation. The CTB, AV or ST reaction mix was added to 30 μL equivalent of Dynabeads M280 Streptavidin (Thermo Fisher Scientific, Waltham, MA) that were pre-washed as per manufacturer's instruction. The reaction mix and beads were incubated at 37°C with shaking at 800 rpm for 30 minutes. The beads were immobilized with a magnet and the supernatant was collected as the "unbound" fraction. The beads were then washed twice with 100 μL wash buffer (0.1% BSA in PBS) and the supernatants were collected as "wash 1" and "wash 2," respectively. The beads were re-suspended in 100 μL PBS as the "bound" fraction. The equivalent of 20% of the starting samples (input) and each of their respective "unbound," "wash 1," "wash 2" and "bound"

Citation: Journal of Extracellular Vesicles 2016, **5**: 29828 - http://dx.doi.org/10.3402/jev.v5.29828

fractions were loaded on a 4–12% SDS-polyacrylamide gel for silver staining or western blot hybridization.

CTB or AV coupled CD81 ELISA

Ten μg of MSC EV was extracted first with 0.25 μg biotinylated CTB or AV, and the remaining supernatant was then extracted with 0.25 μg biotinylated AV or CTB, respectively. Each extraction was performed as described above in a binding buffer at a final volume of 100 μL for 30 minutes, followed by immobilization using 30 μL equivalent of pre-washed Dynabeads M280 Streptavidin. The beads were then washed twice with 100 μL wash buffer (0.1% BSA in PBS), incubated with 100 μL of 1:500 diluted anti-CD81 antibodies (Santa Cruz, CA), washed and incubated again with 1:5,000 diluted HRP-conjugated goat anti-mouse secondary antibodies. HRP activity was determined using Amplex Red Substrate (Life Technology, Grand Island, NY) as per manufacturer's protocol.

Isolation and detection of RNA

CTB-, AV- or ST-binding EVs were each isolated from 200 μg MSC EV using 1.5 μg biotinylated CTB, AV or ST, respectively, in a final volume of 200 μL and the equivalent of 150 μL pre-washed Dynabeads M280 Streptavidin as described above. The isolated EVs were resuspended in 100 μL of PBS and extracted for RNA using 3 volumes of Trizol LS (Thermo Fisher Scientific, Waltham, MA) according to the manufacturer's protocol. After extraction, the pellet was re-suspended in 50 μL RNase-free water. The pellet was assayed for RNA using Quanti-TTM RiboGreen RNA Assay Kit (Thermo Fisher Scientific, Waltham, MA); 10 μL of each resuspended pellet was resolved on a 15% Novex Tris-borate-EDTA (TBE)-urea gels (Thermo Fisher Scientific, Waltham, MA) before staining with ethidium bromide.

Nanoparticle Tracking Analysis

The size distribution of exosome was measured using NanoSight LM10 coupled with a 405-nm laser (Malvern, Worcestershire, UK) and analysed by Nanoparticle Tracking Analysis 2.3 software (Malvern, Worcestershire, UK). MSC-EV preparation was diluted to 2 μg/mL with 0.22 μm filtered PBS and loaded using the NanoSight syringe pump and script control system set at 100 arbitrary units as recommended by NanoSight. Three 30-second videos were recorded at an ambient temperature of 20–21°C with a 10-second delay between recordings. The minimal expected particle size, minimum track length and blur setting were set to the automatic default setting. Camera shutter speed was fixed at 30.00 ms, camera gain at 500, and camera sensitivity and detection threshold at 10. The size and number of particles of the exosome was calculated as the average of 3 replicate recordings.

Electron microscopy

MSC EV (100 μg) preparation was incubated with 1.25 μg biotinylated CTB, AV, ST or without ligand in binding buffer described previously at a final volume of 100 μL for 30 minutes with rotation; 50 μL streptavidin-coated polystyrene particles (Spherotech, Lake Forest, IL) that were pre-washed as per manufacturer's instruction were added to the CTB, AV or ST reaction mix and incubated with shaking at 800 rpm for 30 minutes. The beads were then washed twice with 100 μL PBS and resuspended in 100 μL PBS; 20 μL of each of the bead extracts were spotted directly onto carbon tape on aluminium stubs, and left to dry at 40°C. The stubs were sputter coated with 2 ηm of gold coating (Leica Biosystems Wetzlar, Germany) and imaged in a Jeol 6701FESEM.

Confocal microscopy

Cells were cultured on 20 × 20 mm glass coverslips. At 80% confluence, they were fixed with 4% paraformaldehyde for 15 minutes and then permeabilized with 0.5% Tween 20 for 10 minutes. To reduce background signals from endogenous biotin and other non-specific binding sites, the cells were treated with Endogenous Biotin-Blocking Kit (Thermo Fisher Scientific, Waltham, MA), according to the manufacturer's instructions, followed by StartingBlock T20 (PBS) Blocking Buffer (Thermo Fisher Scientific, Waltham, MA) for 15 minutes. They were then incubated with 5 μg/mL of biotinylated CTB, AV or ST, together with 1:100 diluted anti-CD81 mouse monoclonal IgG_1 antibodies (Santa Cruz Biotechnology, Dallas, TX) at 4°C overnight. Cells were subsequently washed and incubated with 1:50 diluted Streptavidin-Cy3 (Thermo Fisher Scientific, Waltham, MA) with 1:500 diluted Alexa Fluor 488-conjugated goat anti-mouse IgG antibodies (Thermo Fisher Scientific, Waltham, MA) for 1 hour at room temperature. They were then washed, counter-stained with Hoechst 33342, mounted and visualized using a Zeiss LSM 510 laser scanning confocal microscope (Carl Zeiss, Inc., Oberkochen, Germany).

Small RNA sequencing

ST-EV was prepared from 200 μg MSC EV as described above using Trizol LS (Thermo Fisher Scientific, Waltham, MA) according to the manufacturer's protocol. The extracted RNAs were quantitated using Quanti-TTM RiboGreen RNA Assay Kit (Thermo Fisher Scientific, Waltham, MA). One μg RNA each from unfractionated MSC EV preparation and ST-EVs was used for library construction. The library for high-throughput sequencing was constructed using TruSeq Small RNA Library Prep Kit (Cat. #RS-200-0024) and applied to an Illumina High Seq 2000 sequencing system (Illumina, USA) for 101-nt single-end sequencing. The reads obtained were trimmed of their ligation adaptors and reads shorter than 18 nts were discarded. The remaining reads were mapped

against a collection of human rRNA sequences to filter out ribosomal RNA-like reads. The unmapped reads were subsequently mapped to Reference genome hg19 from the UCSC genome browser (www.genome.ucsc.edu/). The ENSEMBL gene annotation (GRCh37) was used to annotate the mapped reads based on its genomic location. For details of the analysis method, please refer to "Supplementary Material and Method."

Western blot hybridization

Western blot hybridization was performed using standard protocols. Briefly, proteins were denatured, separated on 4–12% polyacrylamide gels, electroblotted onto a nitrocellulose membrane and probed with a primary antibody followed by horseradish peroxidase-coupled secondary antibodies against the primary antibody. The primary antibodies used in this study were mouse anti-human CD9, CD81, ALIX, TSG101, CD59, β-ACTIN (Santa Cruz Biotechnology, Dallas, TX) and EDA-containing FN1 (Abcam, Cambridge, MA). After incubating with the appropriate horseradish peroxidase-coupled secondary antibodies, the blot was then incubated with a chemiluminescent HRP substrate to detect bound primary antibody, and therefore the presence of the antigen.

Staurosporine-treated MSC culture

10^5 E1-MYC 16.3 cells were plated into each well of a 6-well culture plate. After 72 hours incubation, the cells were incubated in serum-free chemically defined medium (9) with or without 1 μM staurosporine (Sigma, St Louis, USA) for 3 hours. The culture medium was then harvested and concentrated using a 30 kDa MWCO filter (Merck Millipore, Billerica, MA); 50 μg of the concentrated medium was extracted with AV and the extracts were analysed by western blotting for CD9 and β-ACTIN.

Results

Proteome analysis of CTB-EVs

We have previously described the presence of CTB-EVs in our MSC EV preparation. These EVs were shown by pulse-chase experiments to be derived from endosomes and were therefore bona fide exosomes (5). In addition, CTB could be used to extract endosome-derived MSC EVs from an MSC-conditioned medium. These CTB-EVs carried exosome-associated proteins and had a flotation density of 1.09–1.17 g/mL. In our extraction protocol, CTB effectively extracts at least 96% of CD81 in the conditioned medium (5). Here, we determine the proteome of these CTB-EVs and CTB-EV depleted MSC EV preparation by mass spectrometry as previously described (10). 1,806 proteins were detected in the CTB-bound fraction and 1,547 were present in the CTB-depleted fraction (Supplementary File 1). 987 proteins were found in both fractions, suggesting that these 987 proteins are likely proteins commonly found in most EVs. The observation that 819 and 560 proteins were detected only in either CTB-bound or -depleted fraction respectively indicated that CTB-EVs represent a distinct class of EVs and that there were possibly other EV types beside the CTB-bound EVs (Fig. 1a). The proteins in the CTB-bound fraction and CTB-depleted fraction were functionally clustered into biological process, molecular functions and pathways by the Ingenuity Pathway Analysis platform (Ingenuity Systems, Mountain View, CA). From the analysis of the CTB-bound fraction and CTB-depleted fraction, we respectively selected a set of 20 pathways that had the least likelihood of the clustered proteins being associated with a pathway due to random chance, that is, the lowest p value. There were many shared pathways in these 2 sets. There were also pathways that were unique to either the CTB-bound or depleted fractions (Fig. 1b).

Among the top 20 pathways for the CTB-bound fraction, 4 were endocytic or exocytic processes, namely Caveolar-mediated Endocytosis Signaling, Virus Entry via Endocytic Pathways, Mechanisms of Viral Exit from Host Cells and Clathrin-mediated Endocytosis Signaling. As these pathways essentially function to facilitate endocytosis, endosome-associated activities or exocytosis, their presence were consistent with our previous report that CTB-binding EVs from MSCs have an endosomal origin and were thus exosomes (5). Since endocytosis also plays a critical role in cell adhesion regulation by degrading and recycling cell adhesion molecules such as integrins (11) or ephrins (12), the dominance of cell-adhesion regulatory pathways such as Remodeling of Epithelial Adherens Junctions, Epithelial Adherens Junction Signaling, Germ Cell-Sertoli Cell Junction Signaling, Sertoli Cell-Sertoli Cell Junction Signaling, Ephrin Receptor Signaling and Integrin Signaling could be a coincidental presence in the proteome of endosome-derived CTB-EVs (13–15). However, we postulate that the dominating presence of both endocytosis- and cell-adhesion-associated pathways is not coincidental but rather integral to the biogenesis of exosome. Consistent with this hypothesis, many pathways regulating cytoskeletal biomechanics, which is critical to the membrane restructuring and intracellular membrane vesicle trafficking during endocytosis and cell adhesion, are also dominant in the proteome of CTB-EVs their significant clustering in Actin Cytoskeleton Signaling, and Actin Nucleation by ARP-WASP Complex pathways. Axonal Guidance Signaling, which involves cytoskeleton rearrangement and the modulation of cell-adhesion molecules (17), is also implicated by the CTB-EV proteome. Also, consistent with the central role of endocytosis in the biogenesis of exosomes, several of the cell signal transduction pathways featured in the functional clustering of the CTB-EV proteome shared a common regulatory function in endocytosis, namely 14-3-3-mediated Signaling, PI3K/AKT Signaling, Paxillin Signaling (18,19).

Citation: Journal of Extracellular Vesicles 2016, **5**: 29828 - http://dx.doi.org/10.3402/jev.v5.29828

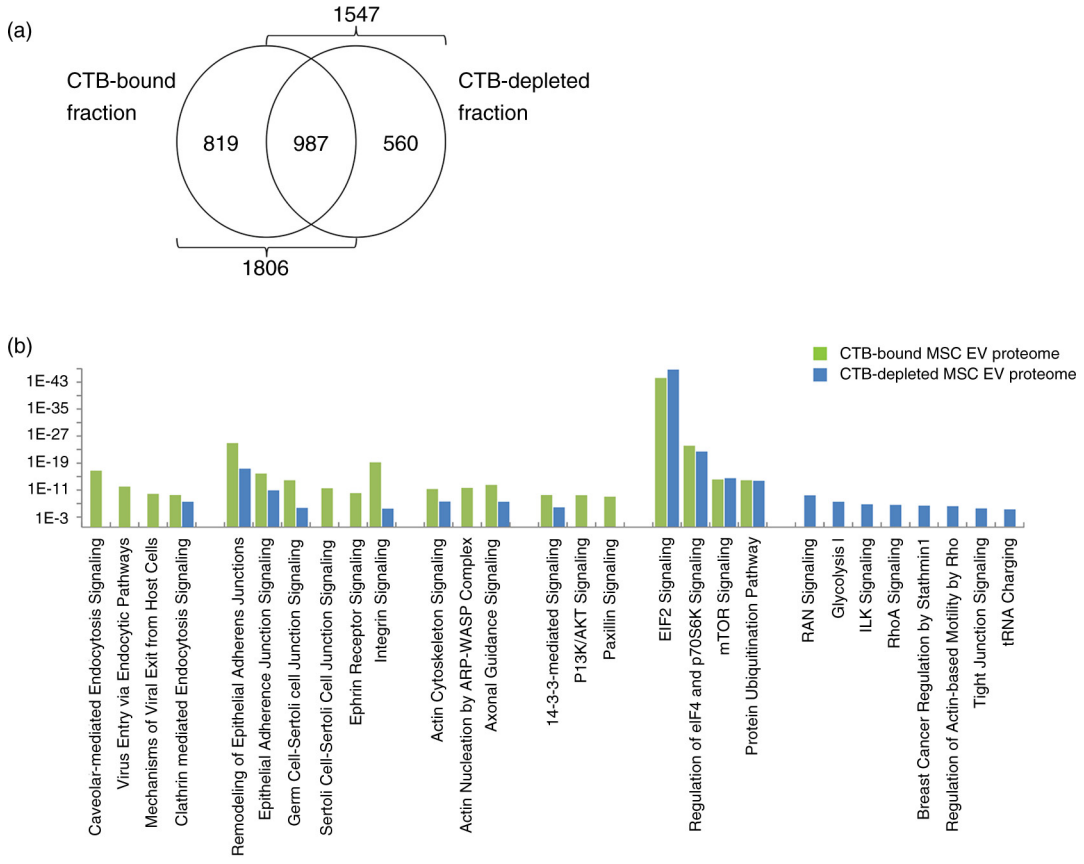

Fig. 1. (a) Proteomic distribution of CTB-EVs and CTB-EV depleted MSC EV preparation by mass spectrometry. 1,806 proteins were detected in the CTB-bound fraction and 1,547 were present in the CTB-depleted fraction. 987 proteins were found in both fractions. (b) Functional clustering of the proteins in the CTB-bound fraction and CTB-depleted fraction.

Another prominent cluster of pathways consists of EIF2 Signaling, Regulation of eIF4 and p70S6K Signaling, mTOR Signaling and Protein Ubiquitination Pathway, which are highly important pathways in protein synthesis, post-translational modifications and translocations that span several subcellular compartments, such as endoplasmic reticulum (ER), Golgi cisternae, the trans-Golgi network (TGN), various types of secretory vesicle and the plasma membrane (20,21). These pathways are consistent with the role of endosomes in protein synthesis and secretion (22,23).

Although the proteome of the MSC CTB-EVs functionally clustered in pathways that could be linked to the endosomal biogenesis of exosomes, many of these links are hypothetical and will have to be validated. It is possible that many of the pathways implicated in the biogenesis also contribute to the biological potency of the EV cargo.

Comparative proteomic analysis of MSC CTB-, AV- and ST-EVs

As the proteomic analysis of MSC CTB-EVs suggested the presence of other EV types, the MSC EV preparation was test extracted with known and commercially available membrane lipid-binding proteins or antibodies. Several ligands were tested, but only AV and ST extract EV types that were different from each other and from CTB-EVs. The extracts were resolved by SDS-PAGE and the gel was stained for proteins (Fig. 2a). Despite the low resolution of the 1D gels, differences among CTB, AV and ST extracts were discernible. These protein differences among the 3 extracts signified that each of the membrane lipid-binding ligands extracted lipids that are complexed with a different cargo of proteins.

To confirm that CTB, AV and ST were extracting EVs, MSC EVs were extracted with each of the 3 ligands. The extracts were then immobilized on streptavidin-conjugated polystyrene beads and visualized by scanning electron microscopy (EM) (Fig. 2c). All 3 EV types were spherical and have approximate sizes of 50–100 ηm. This was consistent with the Nanoparticle Tracking Analysis (NTA) of the EV preparation prior to the ligand extraction. The modal size of EVs in MSC EV preparation was 102 ± 4.8 ηm (Fig. 2b). The spherical shape of the EVs was likely distorted by their immobilization on surfaces with relatively deep crevices and the sample preparation processes. Additionally, their sizes were probably underestimated because the samples had to be dehydrated during preparation for EM analysis.

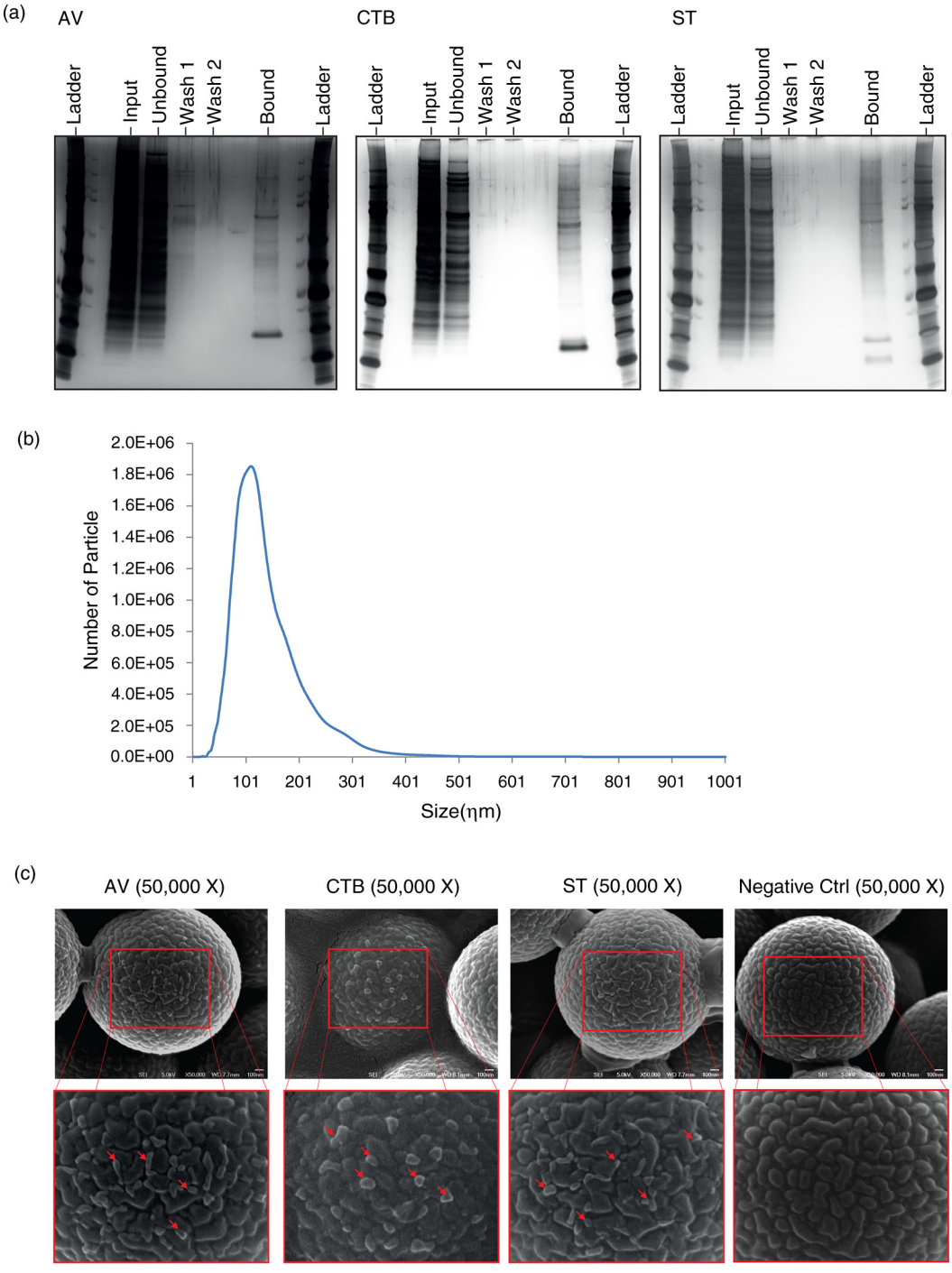

Fig. 2. (a) SDS-PAGE analysis of MSC EVs extracted with membrane lipid-binding ligands, CTB, AV and ST, respectively. MSC CM was incubated with CTB, AV or ST followed by incubation with Dynabeads conjugated with Streptavidin. The beads were immobilized with a magnet and the supernatant was collected as the "unbound" fraction. The beads were then washed twice and the wash solutions were collected as "wash 1" and "wash 2," respectively. The beads were re-suspended in PBS as the "bound" fraction. The equivalent of 20% of the starting samples (input) and each of their respective "unbound," "wash 1," "wash 2" and "bound" fractions were resolved onto polyacrylamide gels and the gels were stained with silver. (b) Size distribution of MSC EVs by NanoSight. MSC EVs were diluted 1,000 × with 0.22 μm filtered PBS. The size distribution of exosome was then measured using NanoSight LM10 and analysed by Nanoparticles Tracking Analysis software according to the manufacturer's protocol. (c) SEM analysis of MSC EVs that were extracted with CTB, AV and ST. MSC EV preparation was incubated with biotinylated CTB, AV, ST or without ligand and then streptavidin-coated polystyrene particles. The beads were then washed twice with PBS and resuspended in PBS before being spotted and left to dry onto carbon tape on aluminium stubs at 40°C. The stubs were sputter coated with 2 ηm of gold coating (Leica Biosystems) and imaged in a Jeol 6701FESEM. Scale bar = 100 ηm.

Citation: Journal of Extracellular Vesicles 2016, **5**: 29828 - http://dx.doi.org/10.3402/jev.v5.29828

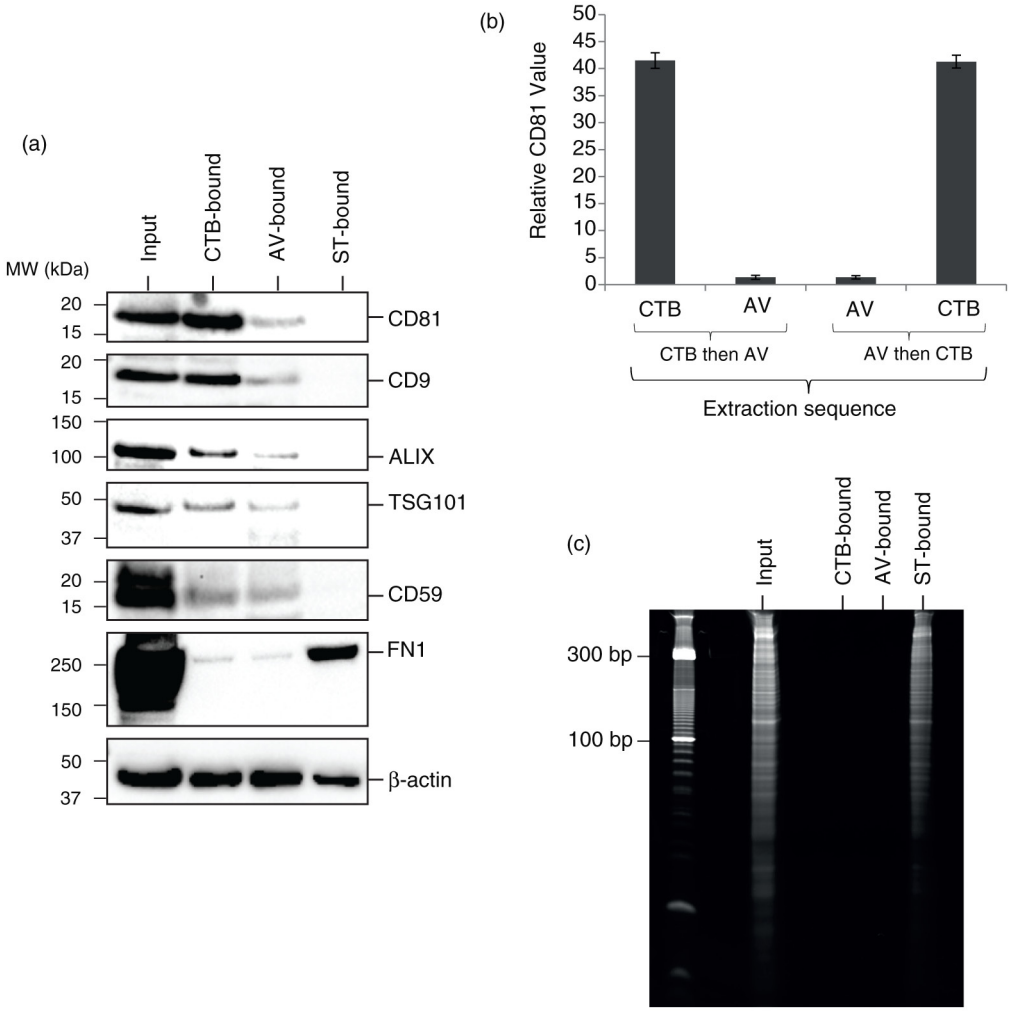

Fig. 3. (a) Western blot analysis of CTB-, AV- and ST-bound MSC EVs. MSC CM was incubated with CTB, AV or ST followed by incubation with Dynabeads conjugated with Streptavidin. The beads were immobilised with a magnet, washed, denatured and resolved onto polyacrylamide gels before electroblotting onto a nitrocellulose membrane. The membrane was probed with a primary antibody followed by horseradish peroxidase-coupled secondary antibodies against the primary antibody. The blot was then incubated with a chemiluminescent HRP substrate to detect bound primary antibody. (b) 10 μg MSC EV was extracted sequentially with biotinylated CTB and then biotinylated AV or vice versa. After each extraction, the ligand-bound vesicles were removed with Dynabeads® MyOne Streptavidin T1 and assayed for CD81 by ELISA. The relative level of CD81 in CTB-vesicles before and after extraction with AV, and that in AV-vesicles before and after extraction with CTB were normalized to that in AV-vesicles before CTB extraction. (c) RNA analysis of CTB-, AV- and ST-EVs. CTB-, AV- or ST-binding EVs were isolated as described above and extracted for RNA using Trizol. The pellet in each of extracts was re-suspended in 50 μL of RNase-free water. 10 μL of each RNA solution was resolved on a 15% Novex Tris-borate-EDTA(TBE)-urea gel before staining with ethidium bromide.

Western blot analysis of the 3 different extracts revealed the presence of actin in all 3 extracts (Fig. 3a). As actin is the most ubiquitous protein in mammalian EVs (24), it is presently the best possible candidate reference protein for comparing relative protein levels among different EVs and was used in this study to compare relative protein levels among the 3 EV types. Exosome-associated proteins such as CD81, CD9, ALIX, and TSG101 were present in the CTB extracts as previously reported (5). Relative to actin, the level of these proteins was very low or not detected in the AV extracts and ST extracts, respectively. To determine whether the low level of exosome-associated proteins in AV-EVs was due to a contamination of CTB-EVs, MSC EVs were first extracted with either CTB or AV and then further extracted with AV or CTB, respectively. The extracted EVs were then assayed for the presence of CD81 by ELISA as previously described (5) (Fig. 3b). The level of CD81 in either CTB- or AV-EVs before and after extraction with AV or CTB, respectively, was not changed, demonstrating that CTB and AV extraction of EVs were mutually exclusive.

Unlike CTB and AV extracts, ST extracts carried detectable level of EDA-containing fibronectin and RNA

(Fig. 3a and c). To confirm the relative RNA distribution in the 3 extracts, the RNA concentration in each extract was assayed by RiboGreen, an RNA fluorescent assay. ST extract had about 53% of the total MSC EV RNA, while both CTB and AV extracts each had less than 0.5% of the total MSC EV RNA.

RNA analysis of ST-binding MSC EVs

To characterize the RNAs in the ST-EVs, RNAs in unfractionated MSC EVs and ST-EVs were sequenced. Two small RNA libraries were generated using RNAs from the unfractionated MSC EVs and ST-EVs. Both libraries generated 204.15 million reads each. After adaptor trimming and the elimination of reads with <18 nts, 117.76 million and 151.13 million reads remained for the ST-EV and unfractionated MSC EVs, respectively. Most of the reads were less than 100 nts, with most reads being less than 40 nt. These reads were then filtered to remove ribosomal RNA-like sequences before mapping to hg19 human genome; 19.9 million of the 35.71 million reads in ST-EV and 17.8 million of the 46.05 million reads in unfractionated MSC EVs were miscellaneous RNAs, that is, non-coding RNAs that cannot be categorized by ENSEMBL. The vast majority of miscellaneous RNA identified are a small non-coding RNA component of soluble ribonucleoproteins (RNPs) (Supplementary File 3). The top 5 expressed misc_RNA in both unfractionated MSC EVs and ST-EVs were Y RNAs. According to NCBI (www.ncbi.nlm.nih.gov/gene/6084), Y RNAs are small non-coding RNAs that are the RNA component of soluble RNPs known as Ro RNPs. Ro RNPs have been associated with rheumatic diseases such as systemic lupus erythematosus and Sjogren syndrome. Qualitatively, the RNAs in ST-EV were different from those in unfractionated MSC EVs. The majority of RNAs in both ST-EV and the unfractionated MSC EVs is ribosomal RNAs. For the rest, the 5 most abundant classes of RNA in the ST-EVs were Y RNA, snRNA, miRNA, lincRNA and protein-coding RNA (Fig. 4a), while the 5 most abundant classes of RNA in the unfractionated MSC EVs were Y RNA, snoRNA, protein-coding RNA, snRNA and processed transcript (Fig. 4b). The top 5 most abundant miRNAs in both preparation are mir-191, mir-181, mir-22, mir-92 and mir-221 (Supplementary Fig. 1, The TPM (tags per million) of miRNAs can be found in Supplementary File 2). Therefore, it is possible that ST-EVs are not the only RNA-containing EVs in the MSC EV preparation.

Steady-state AV-EVs are different from AV-EVs produced during apoptosis

As AV-EVs must have exposed phosphatidylserines to bind AV, there is a good possibility that they might be derived from apoptotic cells. We tested this by inducing apoptosis in our MSC culture with staurosporine. In healthy MSC culture, most of the CD9 was associated with CTB-EVs, while AV-EVs contained low or undetectable levels of CD9. However, during apoptosis, the level of CD9 relative to actin was elevated by 3.8 fold (Fig. 5), suggesting that the composition of AV-EVs produced by healthy MSCs was different from that by apoptotic MSCs, and more exosome-associated markers were being secreted in AV-EVs during apoptosis. As such, CTB may be a more stable ligand for extracting exosomes than exosome-associated markers such as CD9.

Candidate cellular origin of CTB-, AV- and ST-EVs

The different membrane lipid affinities and cargos of CTB-, AV- and ST-EVs indicated that they were likely to be different EV types derived from either different domains of the plasma membrane or different membrane organelles. To identify the candidate membrane sources of these EVs, MSCs were stained with fluorescence-labelled CTB, AV and ST. CTB binding activity was localized to the discrete domains on the plasma membrane and cytoplasm, AV binding activity was diffused throughout the cytoplasm, and ST binding activity was diffused throughout the nuclei (Fig. 6). To ascertain whether the staining pattern by CTB, AV and ST was specific to MSC or a more general cellular phenomenon, immortalized human keratinocytes (25) and myc-immortalized human myoblasts were tested and found to have similar staining patterns (Fig. 7).

Discussion

In this report, we investigated the EV types present in our previously described MSC exosome preparation (2). This MSC exosome preparation was purified from a chemically defined medium that had been conditioned by MSCs for 3 days and then size-fractionated (3). As described in the "Introduction," we had previously described this preparation as an exosome preparation based on the presence of exosome-associated parameters and properties. We also subsequently demonstrated through pulse-chase experiments that this preparation contained CTB-binding EVs that were derived from endosomes (5). Here, we report that these CTB-EVs had a proteome enriched in proteins that were functionally important in the cellular process of endocytosis. However, this elucidation of the proteome of CTB-EVs by mass spectrometry also revealed that this proteome constituted only part of the MSC EV proteome, suggesting the presence of other EV types. As such, the previously described MSC exosome preparation was incorrect and should be described as an EV preparation.

To identify the other EV types in MSC EV preparation, 2 ligands, AV and ST known to bind membrane lipids, phosphatidylserine and globotriaosylceramide, respectively, were tested to see whether they would extract the remaining proteins. The rationale for using such ligands was to ensure that the extracted proteins are in a

Citation: Journal of Extracellular Vesicles 2016, **5**: 29828 - http://dx.doi.org/10.3402/jev.v5.29828

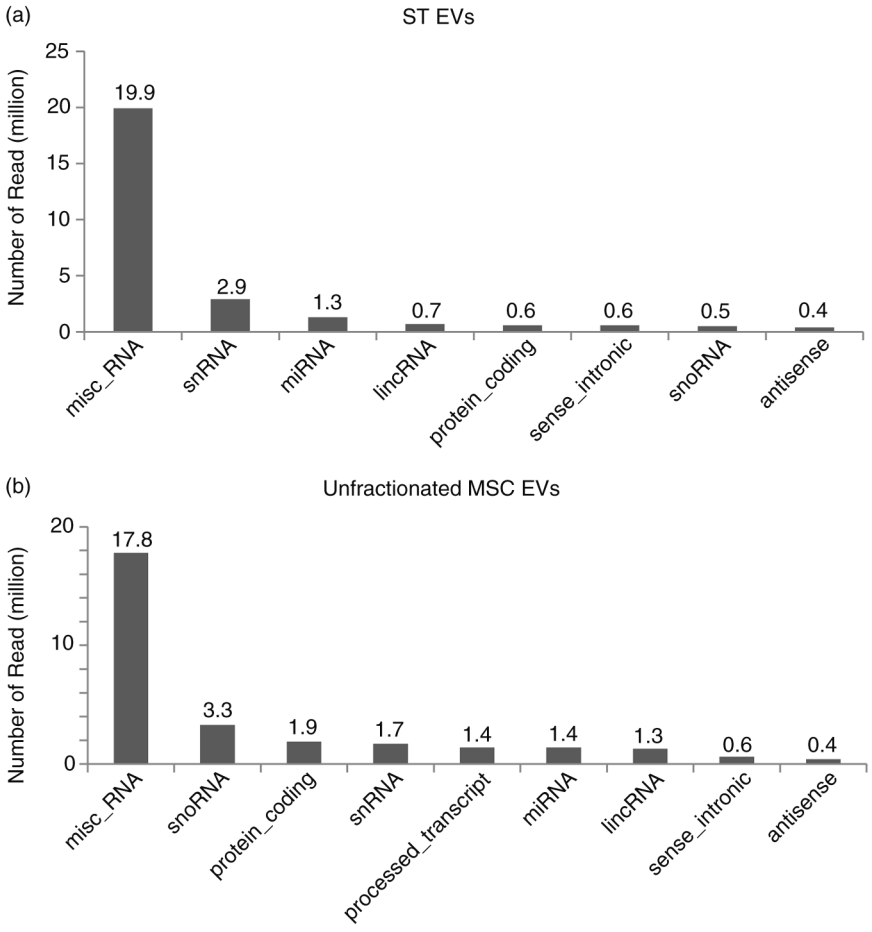

Fig. 4. Sequencing of RNA from MSC EV and ST-EV. 1 μg extracted RNA from the unfractionated MSC EV preparation and ST-EVs was used to construct libraries for sequencing on an Illumina High Seq 2000 sequencing system (Illumina, USA). The ligation adaptors of the reads generated were trimmed. Those reads shorter than 18 nts and ribosomal RNA-like reads were filtered off. The remaining reads were mapped back to genome hg19. The mapped reads were annotated by the ENSEMBL gene annotation (GRCh37). The distribution of the mapped reads across the different RNA types were tabulated for mapped RNA of (a) ST-EV and (b) unfractionated MSC -EVs.

membrane lipid complex. EM visualization of 50–100 ηm vesicle-like structures in each of the extracts indicated that the membrane lipid complexes are vesicles. Like CTB, both AV and ST also extracted proteins. Significantly, CTB and AV extracts contained membrane proteins such as CD9, CD81 and CD59. This property has been highlighted as an important characteristic of membrane vesicles in a position paper by the International Society of Extracellular Vesicles (6).

Visual inspection of proteins extracted by all 3 ligands using low-resolution 1D protein gels revealed discernible differences. Western blot confirmed these differences. Actin, the protein most often found in mammalian EVs (24), was present in all 3 extracts and, as such, was used here as a normalization reference for our experiments. As expected of exosome as EVs with an endosomal biogenesis, CTB extracts had all the known endosomal

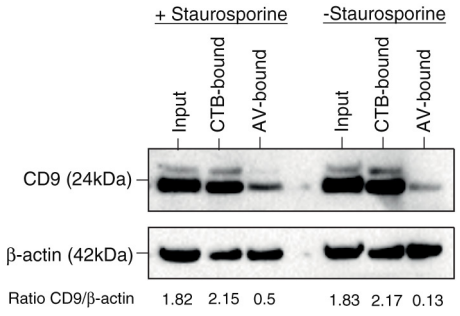

Fig. 5. EVs from steady state versus apoptotic MSC cultures. MSC was cultured in chemically defined medium for 72 hours and then treated with or without 1 μM staurosporine for 3 hours. The media were then harvested and extracted with CTB or AV, and the extracts analysed for CD9 and actin by western blot. The CD9 and actin signals were scanned and the CD9 signal in each extract was normalized to actin.

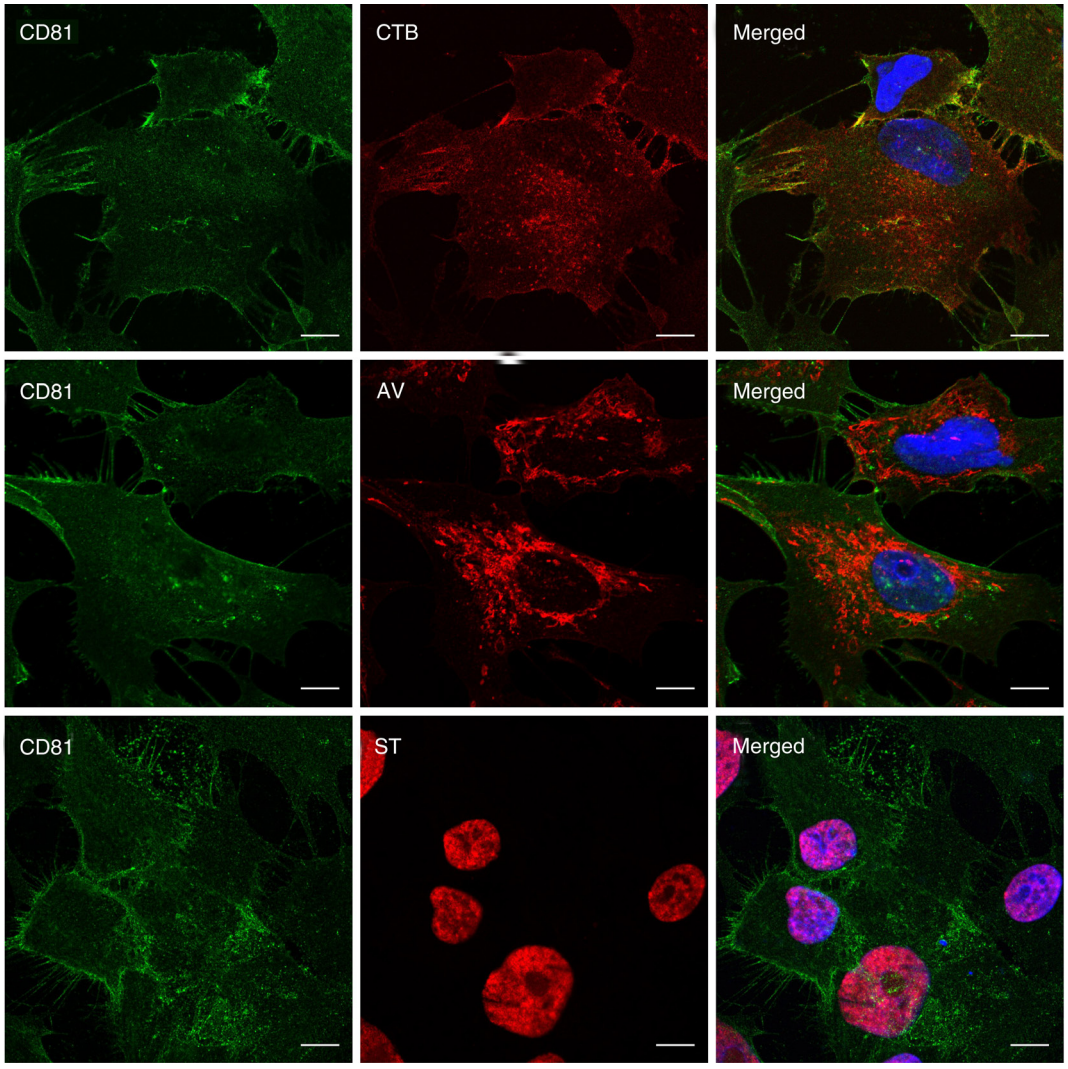

Fig. 6. Visualization of CTB-, AV- and ST-binding in E1-MYC 16.3 cells. Cells were fixed and co-stained with anti-CD81 antibody (green) and labelled CTB, AV or ST (red). They were then counterstained with Hoechst 33342 to visualize the nuclei (blue). Scale bars, 10 μm.

exosome-associated proteins. Although AV-EVs also contained very low levels of exosome-associated proteins, prior extraction with either CTB or AV did not reduce the level of exosome-associated CD81 in AV- or CTB-EVs, respectively. Therefore, AV-EVs cannot be extracted by CTB and vice versa, and AV and CTB extraction are mutually exclusive. In treating permeabilized MSCs with fluorescence-labelled CTB, the CTB-binding activity in MSCs was either confined to specific domains in the plasma membrane or in punctate cytoplasmic distribution in co-localization with CD81 (26), consistent with the biogenesis of endosomes. This cellular distribution of CTB-binding activity could be attributed to the cellular receptor for CTB, namely GM1 ganglioside. GM1 gangliosides are known to be enriched in lipid rafts, which are sites of active endocytosis, and are thus enriched in endosomes as well.

In contrast to CTB-binding activity, AV-binding activity was concentrated mainly in the cytoplasm and did not co-localize with CD81, suggesting that AV-EVs were derived from membrane organelles in the cytoplasm. In the presence of Ca^{2+}, AV is known to have a high specific affinity for phosphatidylserine but in the absence of Ca^{2+}, AV binds phosphatidylcholine (27). Therefore, the staining of the cytoplasm and not the phosphatidylcholine-rich plasma membrane by AV is not an artefact caused by a lack of Ca^{2+}. Although phosphatidylserine is better known as an extracellular cell surface marker for apoptosis, its main subcellular locations and functions are intracellular (review (28)). The organelles known to be most enriched in phosphatidylserine are the plasma membrane, endosomes and secretory vesicles. This subcellular distribution of PS is thus different from our observed subcellular locations of AV-binding activities. We postulate that one possible reason for this discrepancy is the context-dependent AV binding of PS, that is, the presence of other phospholipids, such as phosphatidylethanolamine, could affect the binding

Citation: Journal of Extracellular Vesicles 2016, **5**: 29828 - http://dx.doi.org/10.3402/jev.v5.29828

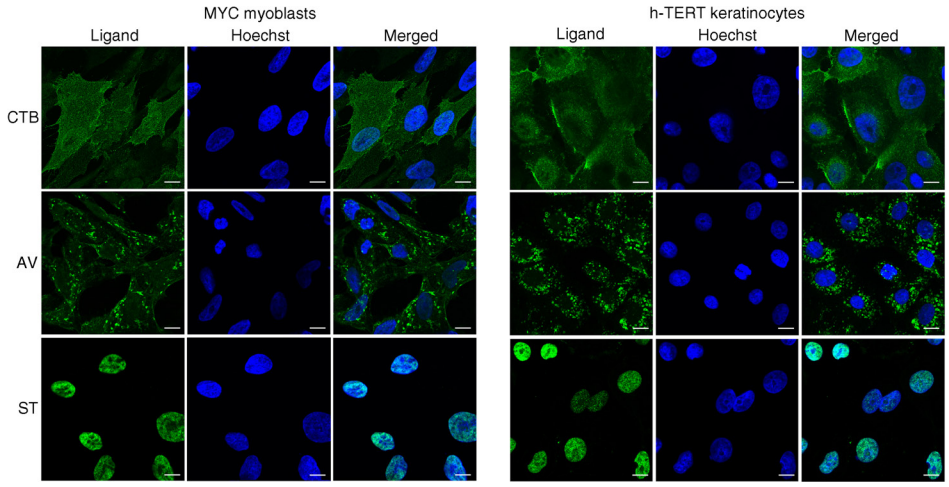

Fig. 7. Visualization of CTB-, AV- and ST-binding in immortalized human skeletal myoblasts and keratinocytes. Cells were fixed and stained with labelled CTB, AV or ST (green), and counterstained with Hoechst 33342 to visualize the nuclei (blue). Scale bars, 10 μm.

of PS by AV (29). Hence, a low abundance PS in the right context may bind AV more efficiently than a high abundance PS in a poor context. Another possible reason is that unlike antibodies, all 3 ligands, that is, CTB, AV and ST, bind multiple copies of their lipid ligands. One AV molecule binds 4–8 PS molecule (30,31), while both CTB and ST are pentamers in which one CTB monomer binds one GM1 (32), and one ST monomer binds one or more GB3 (33). As such, the cellular locations of CTB, AV and ST binding activity highlight only those locations in which their lipid ligands are highly enriched in sufficiently close physical proximity for polyvalent binding. As such, the efficacy or efficiency of CTB, AV or ST in extracting EVs is highly dependent on the spacing and density of their lipid ligands. It cannot be predicted simply by the presence or absence of the lipids in the EV membrane. Based on the cytoplasmic distribution of AV-binding sites, the biogenesis pathway of AV-EVs is likely to either physically or biochemically intersect with that of CTB-EVs, which would provide a rationale for some of the proteomic intersect of AV- and CTB-EVs, as evidenced by the low level of CD9, CD81, Alix Tsg101 and CD59 relative to actin

Of the 3 EVs, ST-EVs were uniquely different not only in their cargo of RNA and EDA-fibronectin but also in the cellular distribution of their binding activity, which was restricted to the nucleus. We had previously reported that RNAs secreted by MSC were less than 300 nts and were encapsulated in cholesterol-rich phospholipid vesicles (4). These RNAs were susceptible to RNAse activity only after pre-treatment with detergent, phospholipase A2 or cyclodextrin a chelator of cholesterol. They also have a low EV-like buoyant density of 1.1 g/mL and this buoyant density could be increased towards a more RNA-like buoyant density by treatment with a combination of phospholipase A2 and cyclodextrin (1.13–1.16 g/mL) or an SDS-based lysis buffer (1.15–1.18 g/mL). This increase in apparent RNA density by lipid extraction treatments demonstrates that the RNA is in a lipid complex such that the removal of less dense lipids increase their apparent density. Until now, there are no evidence to suggest that RNA-containing EVs from MSCs were physically different from other EVs. ST-EVs carry at least 50% of the total MSC EV RNA, while both CTB-and AV-EVs each carry less than 0.5%. Therefore, any EV RNA-mediated biological activity is likely to reside with ST-EVs, and not CTB-and AV-EVs. Although this nuclear location of the binding site could provide a rationale for its RNA cargo, the biogenesis and the biological significance of ST-EVs, its cargo of relatively short and seemingly non-functional RNAs, and its cargo of fibronectin, an extracellular protein, are enigmatic from our present perspective of EV biogenesis and functions. To date, biogenesis of EVs from the nucleus has not been described and no currently known biological process or processes could provide a mechanistic model for the biogenesis of EVs that involves both nuclear materials and extracellular matrix proteins.

In summary, MSC produces at least 3 distinct 100 ηm EV types, CTB-, AV- and ST-EVs, that could be distinguished by their membrane lipid composition, their proteome and RNA cargo. The unique presence of RNA and fibronectin in ST-EVs and the mutually exclusive EV binding activity of CTB and AV demonstrate that these 3 EV types are unique entities. Based on the different subcellular location of CTB-, AV- and ST-binding activities in MSCs and other cell types, these EV types are likely to have a different biogenesis. However, the biological significance and functions of these different EV types remains to be elucidated. Nevertheless, the identification of these diverse EV types provides the initial key in stratifying and clarifying the diverse and often disparate biological functions that had been attributed to EVs in general.

Acknowledgements

We gratefully acknowledge Jayanthi Padmanabhan (BTI) for the preparation of the conditioned medium and purification of the exosomes and Dr Adrian Hui Kuang Boey (IMB-IMCB Joint Electron Microscopy Suite, A*STAR Singapore) for assistance in preparing and imaging specimens for this research.

Conflict of interest and funding

The authors declare no conflict of interest and have not received any funding or benefits from industry or any for profit organization for this work.

References

1. Yeo RW, Lai RC, Zhang B, Tan SS, Yin Y, Teh BJ, et al. Mesenchymal stem cell: an efficient mass producer of exosomes for drug delivery. Adv Drug Deliv Rev. 2013;65:336–41.
2. Timmers L, Lim S-K, Arslan F, Armstrong JS, Hoefler IE, Doevendans PA, et al. Reduction of myocardial infarct size by human mesenchymal stem cell conditioned medium. Stem Cell Res. 2008;1:129–37.
3. Lai RC, Arslan F, Lee MM, Sze NS, Choo A, Chen TS, et al. Exosome secreted by MSC reduces myocardial ischemia/reperfusion injury. Stem Cell Res. 2010;4:214–22.
4. Chen TS, Lai RC, Lee MM, Choo AB, Lee CN, Lim SK. Mesenchymal stem cell secretes microparticles enriched in pre-microRNAs. Nucleic Acids Res. 2010;38:215–24.
5. Tan SS, Yin Y, Lee T, Lai RC, Yeo RW, Zhang B, et al. Therapeutic MSC exosomes are derived from lipid raft microdomains in the plasma membrane. J Extracell Vesicles. 2013;2:22614, doi: http://dx.doi.org/10.3402/jev.v2i0.22614
6. Lotvall J, Hill AF, Hochberg F, Buzas EI, Di Vizio D, Gardiner C, et al. Minimal experimental requirements for definition of extracellular vesicles and their functions: a position statement from the international society for extracellular vesicles. J Extracell Vesicles. 2014;3:26913, doi: http://dx.doi.org/10.3402/jev.v3.22913
7. Chen TS, Arslan F, Yin Y, Tan SS, Lai RC, Choo AB, et al. Enabling a robust scalable manufacturing process for therapeutic exosomes through oncogenic immortalization of human ESC-derived MSCs. J Transl Med. 2011;9:47.
8. Lai RC, Arslan F, Tan SS, Tan B, Choo A, Lee MM, et al. Derivation and characterization of human fetal MSCs: an alternative cell source for large-scale production of cardioprotective microparticles. J Mol Cell Cardiol. 2010;48:1215–24.
9. Sze SK, de Kleijn DP, Lai RC, Tan EKW, Zhao H, Yeo KS, et al. Elucidating the secretion proteome of human embryonic stem cell-derived mesenchymal stem cells. Mol Cell Proteomics. 2007;6:1680–9.
10. Lai RC, Tan SS, Teh BJ, Sze SK, Arslan F, de Kleijn DP, et al. Proteolytic potential of the MSC exosome proteome: implications for an exosome-mediated delivery of therapeutic proteasome. Int J Proteomics. 2012;2012:971907.
11. Caswell PT, Vadrevu S, Norman JC. Integrins: masters and slaves of endocytic transport. Nat Rev Mol Cell Biol. 2009;10:843–53. doi: http://dx.doi.org/10.1038/nrm2799
12. Pitulescu ME, Adams RH. Eph/ephrin molecules—a hub for signaling and endocytosis. Gene Dev. 2010;24:2480–92.
13. Kopera IA, Bilinska B, Cheng CY, Mruk DD. Sertoli-germ cell junctions in the testis: a review of recent data. Philos Trans R Soc Lond B Biol Sci. 2010;365:1593–605.
14. Yan HH, Mruk DD, Wong EW, Lee WM, Cheng CY. An autocrine axis in the testis that coordinates spermiation and blood-testis barrier restructuring during spermatogenesis. Proc Natl Acad Sci USA. 2008;105:8950–5.
15. Delva E, Kowalczyk AP. Regulation of cadherin trafficking. Traffic. 2009;10:259–67.
16. Welch MD, Mullins RD. Cellular control of actin nucleation. Annu Rev Cell Dev Biol. 2002;18:247–88.
17. Bashaw GJ, Klein R. Signaling from axon guidance receptors. Cold Spring Harb Perspect Biol. 2010;2:a001941.
18. Sorkin A, von Zastrow M. Endocytosis and signalling: intertwining molecular networks. Nat Rev Mol Cell Biol. 2009;10:609–22.
19. Schiefermeier N, Teis D, Huber LA. Endosomal signaling and cell migration. Curr Opin Cell Biol. 2011;23:615–20.
20. Buszczak M, Signer Robert AJ, Morrison Sean J. Cellular differences in protein synthesis regulate tissue homeostasis. Cell. 2014;159:242–51.
21. Bonifacino JS, Rojas R. Retrograde transport from endosomes to the trans-Golgi network. Nat Rev Mol Cell Biol. 2006;7:568–79.
22. Lodish H BA, Zipursky SL, et al. Section 17.3, Overview of the secretory pathway. Molecular cell biology. 4th ed. New York: W.H. Freeman; 2000.
23. Alberts B JA, Lewis J, et al. Transport into the cell from the plasma membrane: endocytosis. Molecular biology of the cell. 4th ed. New York: Garland Science; 2002.
24. Choi D-S, Kim D-K, Kim Y-K, Gho YS. Proteomics of extracellular vesicles: exosomes and ectosomes. Mass Spectrom Rev. 2015;34:474–90.
25. Dickson MA, Hahn WC, Ino Y, Ronfard V, Wu JY, Weinberg RA, et al. Human keratinocytes that express hTERT and also Bypass a p16(INK4a)-Enforced mechanism that limits life span become immortal yet retain normal growth and differentiation characteristics. Mol Cell Biol. 2000;20:1436–47.
26. Lai RC, Chen TS, Lim SK Mesenchymal stem cell exosome: a novel stem cell-based therapy for cardiovascular disease. Regenerative medicine. 2011;6(4):481–92.
27. Maffey KG, Keil LB, DeBari VA. The Influence of lipid composition and divalent cations on annexin v binding to phospholipid mixtures. Ann Clin Lab Sci. 2001;31:85–90.
28. Leventis PA, Grinstein S. The distribution and function of phosphatidylserine in cellular membranes. Annu Rev Biophys. 2010;39:407–27.
29. Lizarbe M, Barrasa J, Olmo N, Gavilanes F, Turnay J. Annexin-phospholipid interactions. Functional implications. Int J Mol Sci. 2013;14:2652.
30. Meers P, Mealy T. Calcium-dependent annexin V binding to phospholipids: stoichiometry, specificity, and the role of negative charge. Biochemistry. 1993;32:11711–21.
31. Sopkova J, Renouard M, Lewit-Bentley A. The crystal structure of a new high-calcium form of annexin V. J Mol Biol. 1993;234:816–25.
32. Merritt EA, Sarfaty S, van den Akker F, L'Hoir C, Martial JA, Hol WG. Crystal structure of cholera toxin B-pentamer bound to receptor GM1 pentasaccharide. Protein Sci. 1994;3:166–75.
33. Ling H, Boodhoo A, Hazes B, Cummings MD, Armstrong GD, Brunton JL, et al. Structure of the shiga-like toxin I B-pentamer complexed with an analogue of its receptor Gb3. Biochemistry. 1998;37:1777–88.